Research Article
Vol. 26, No. 3 | 5 Feb 2018 | OPTICS EXPRESS 2325
Optics EXPRESS

Rate equation modeling of the frequency noise and the intrinsic spectral linewidth in quantum cascade lasers

XING-GUANG WANG,[1] FRÉDÉRIC GRILLOT,[2,3] AND CHENG WANG[1,*]

[1]*School of Information Science and Technology, ShanghaiTech University, Shanghai 201210, China.*
[2]*LTCI, Télécom ParisTech, Université Paris Saclay, 46 rue Barrault, F-75634 Paris Cedex 13, France*
[3]*Center for High Technology Materials, University of New Mexico, 1313 Goddard SE, Albuquerque, New Mexico 87106-4343, USA*
[*]*wangcheng1@shanghaitech.edu.cn*

Abstract: This work theoretically investigates the frequency noise (FN) characteristics of quantum cascade lasers (QCLs) through a three-level rate equation model, which takes into account both the carrier noise and the spontaneous emission noise through the Langevin approach. It is found that the power spectral density of the FN exhibits a broad peak due to the carrier noise induced carrier variation in the upper laser level, which is enhanced by the stimulated emission process. The peak amplitude is strongly dependent on the gain stage number and the linewidth broadening factor. In addition, an analytical formula of the intrinsic spectral linewidth of QCLs is derived based on the FN analysis. It is demonstrated that the laser linewidth can be narrowed by reducing the gain coefficient and/or accelerating the carrier scattering rates of the upper and the lower laser levels.

OCIS codes: (140.5965) Semiconductor lasers, quantum cascade; (270.2500) Fluctuations, relaxations, and noise; (290.3700) Linewidth.

References and links

1. J. Faist, F. Capasso, D. L. Sivco, C. Sirtori, A. L. Hutchinson, and A. Y. Cho, “Quantum cascade laser,” Science **264**(5158), 553–556 (1994).
2. J. Faist, *Quantum Cascade Lasers* (Oxford, 2013).
3. A. A. Kosterev and F. K. Tittel, “Chemical sensors based on quantum cascade lasers,” IEEE J. Quantum Electron. **38**(6), 582–591 (2002).
4. A. Kosterev, G. Wysocki, Y. Bakhirkin, S. So, R. Lewicki, M. Fraser, F. Tittel, and R. F. Curl, “Application of quantum cascade lasers to trace gas analysis,” Appl. Phys. B **90**(2), 165–176 (2008).
5. S. W. Sharpe, J. F. Kelly, J. S. Hartman, C. Gmachl, F. Capasso, D. L. Sivco, J. N. Baillargeon, and A. Y. Cho, “High-resolution (Doppler-limited) spectroscopy using quantum-cascade distributed-feedback lasers,” Opt. Lett. **23**(17), 1396–1398 (1998).
6. H.-W. Hübers, S. G. Pavlov, H. Richter, A. D. Semenov, L. Mahler, A. Tredicucci, H. E. Beere, and D. A. Ritchie, “High-resolution gas phase spectroscopy with a distributed feedback terahertz quantum cascade laser,” Appl. Phys. Lett. **89**(6), 061115 (2006).
7. A. W. M. Lee, B. S. Williams, S. Kumar, Q. Hu, and J. L. Reno, “Real-time imaging using a 4.3-THz quantum cascade laser and a 320×240 microbolometer focal-plane array,” IEEE Photonics Technol. Lett. **18**(13), 1415–1417 (2006).
8. R. Martini, C. Bethea, C. Gmachl, R. Paiella, E. A. Whittacker, H. Y. Hwang, D. L. Sivco, J. N. Baillargeon, and A. Y. Cho, “Free-space optical transmission of multimedia satellite data streams using mid-infrared quantum cascade lasers,” Electron. Lett. **38**(4), 181–183 (2002).
9. P. D. Grant, S. R. Laframboise, R. Dudek, M. Graf, A. Bezinger, and H. C. Liu, “Terahertz free space communications demonstration with quantum cascade laser and quantum well photodetector,” Electron. Lett. **45**(18), 952–954 (2009).
10. A. Hugi, G. Villares, S. Blaser, H. C. Liu, and J. Faist, “Mid-infrared frequency comb based on a quantum cascade laser,” Nature **492**(7428), 229–233 (2012).
11. Y. Takagi, N. Kumazaki, M. Ishihara, K. Kasahara, A. Sugiyama, N. Akikusa, and T. Edamura, “Relative intensity noise measurements of 5 µm quantum cascade laser and 1.55 µm semiconductor laser,” Electron. Lett. **44**(14), 860–861 (2008).
12. F. Rana and R. J. Ram, “Current noise and photon noise in quantum cascade lasers,” Phys. Rev. B **65**(12), 125313 (2002).

#309924 https://doi.org/10.1364/OE.26.002325
Journal © 2018 Received 24 Oct 2017; revised 11 Jan 2018; accepted 11 Jan 2018; published 23 Jan 2018

Optics EXPRESS

13. T. Gensty and W. Elsäßer, "Semiclassical model for the relative intensity noise of intersubband quantum cascade lasers," Opt. Commun. **256**(1–3), 171–183 (2005).
14. T. Gensty, W. Elsäßer, and C. Mann, "Intensity noise properties of quantum cascade lasers," Opt. Express **13**(6), 2032–2039 (2005).
15. D. Weidmann, K. Smith, and B. Ellison, "Experimental investigation of high-frequency noise and optical feedback effects using a 9.7 μm continuous-wave distributed-feedback quantum-cascade laser," Appl. Opt. **46**(6), 947–953 (2007).
16. M. Carras, F. Schad, L. Drzewietzki, S. Breuer, C. Juretzka, and W. Elsäßer, "9.5 dB relative intensity noise reduction in quantum cascade laser by detuned loading," Electron. Lett. **49**(24), 1548–1550 (2013).
17. H. Simos, A. Bogris, D. Syvridis, and W. Elsäßer, "Intensity noise properties of mid-infrared injection locked quantum cascade lasers: I. Modeling," IEEE J. Quantum Electron. **50**(2), 98–105 (2014).
18. C. Juretzka, H. Simos, A. Bogris, D. Syvridis, and W. Elsäßer, "Intensity noise properties of midinfrared injection locked quantum cascade lasers: II. Experiments," IEEE J. Quantum Electron. **51**(1), 2300208 (2015).
19. G. Di Domenico, S. Schilt, and P. Thomann, "Simple approach to the relation between laser frequency noise and laser line shape," Appl. Opt. **49**(25), 4801–4807 (2010).
20. L. A. Coldren, S. W. Corzine, and M. L. Mashanovitch, *Diode Lasers and Photonic Integrated Circuits* (Wiley, 2012).
21. A. Hangauer and G. Wysocki, "Gain compression and linewidth enhancement factor in mid-IR quantum cascade lasers," IEEE J. Sel. Top. Quantum Electron. **21**(6), 1200411 (2015).
22. S. Bartalini, S. Borri, P. Cancio, A. Castrillo, I. Galli, G. Giusfredi, D. Mazzotti, L. Gianfrani, and P. De Natale, "Observing the intrinsic linewidth of a quantum-cascade laser: Beyond the Schawlow-Townes limit," Phys. Rev. Lett. **104**(8), 083904 (2010).
23. L. Tombez, J. Di Francesco, S. Schilt, G. Di Domenico, J. Faist, P. Thomann, and D. Hofstetter, "Frequency noise of free-running 4.6 μm distributed feedback quantum cascade lasers near room temperature," Opt. Lett. **36**(16), 3109–3111 (2011).
24. S. Borri, S. Bartalini, P. C. Pastor, I. Galli, G. Giusfredi, D. Mazzotti, M. Yamanishi, and P. De, "Natale, "Frequency-noise dynamics of mid-infrared quantum cascade lasers," IEEE J. Quantum Electron. **47**(7), 984–988 (2011).
25. L. Tombez, S. Schilt, J. Di Francesco, T. Fuhrer, B. Rein, T. Walther, G. Di Domenico, D. Hofstetter, and P. Thomann, "Linewidth of a quantum cascade laser assessed from its frequency noise spectrum and impact of the current driver," Appl. Phys. B **109**(3), 407–414 (2012).
26. S. Schilt, L. Tombez, G. Di Domenico, and D. Hofstetter, "Frequency noise and linewidth of mid-infrared continuous-wave quantum cascade lasers: An overview," in *The Wonder of Nanotechnology: Quantum Optoelectronic Devices and Applications* (SPIE, 2013).
27. R. M. Williams, J. F. Kelly, J. S. Hartman, S. W. Sharpe, M. S. Taubman, J. L. Hall, F. Capasso, C. Gmachl, D. L. Sivco, J. N. Baillargeon, and A. Y. Cho, "Kilohertz linewidth from frequency-stabilized mid-infrared quantum cascade lasers," Opt. Lett. **24**(24), 1844–1846 (1999).
28. M. S. Taubman, T. L. Myers, B. D. Cannon, R. M. Williams, F. Capasso, C. Gmachl, D. L. Sivco, and A. Y. Cho, "Frequency stabilization of quantum-cascade lasers by use of optical cavities," Opt. Lett. **27**(24), 2164–2166 (2002).
29. F. Bielsa, A. Douillet, T. Valenzuela, J. P. Karr, and L. Hilico, "Narrow-line phase-locked quantum cascade laser in the 9.2 μm range," Opt. Lett. **32**(12), 1641–1643 (2007).
30. S. Borri, I. Galli, F. Cappelli, A. Bismuto, S. Bartalini, P. Cancio, G. Giusfredi, D. Mazzotti, J. Faist, and P. De Natale, "Direct link of a mid-infrared QCL to a frequency comb by optical injection," Opt. Lett. **37**(6), 1011–1013 (2012).
31. B. Argence, B. Chanteau, O. Lopez, D. Nicolodi, M. Abgrall, C. Chardonnet, C. Daussy, B. Darquié, Y. Le Coq, and A. Amy-Klein, "Quantum cascade laser frequency stabilization at the sub-Hz level," Nat. Photonics **9**(7), 456–460 (2015).
32. M. Yamanishi, T. Edamura, K. Fujita, N. Akikusa, and H. Kan, "Theory of the intrinsic linewidth of quantum-cascade lasers: Hidden reason for the narrow linewidth and line-broadening by thermal photons," IEEE J. Quantum Electron. **44**(1), 12–29 (2008).
33. C. Jirauschek, "Monte Carlo study of intrinsic linewidths in terahertz quantum cascade lasers," Opt. Express **18**(25), 25922–25927 (2010).
34. M. Yamanishi, "Theory of intrinsic linewidth based on fluctuation-dissipation balance for thermal photons in THz quantum-cascade lasers," Opt. Express **20**(27), 28465–28478 (2012).
35. T. Liu and Q. J. Wang, "Fundamental frequency noise and linewidth broadening caused by intrinsic temperature fluctuations in quantum cascade lasers," Phys. Rev. B **84**(12), 125322 (2011).
36. T. Liu, K. E. Lee, and Q. J. Wang, "Effects of resonant tunneling and dynamics of coherent interaction on intrinsic linewidth of quantum cascade lasers," Opt. Express **20**(15), 17145–17159 (2012).
37. C. Wang, F. Grillot, V. Kovanis, and J. Even, "Rate equation analysis of injection-locked quantum cascade lasers," J. Appl. Phys. **113**(6), 063104 (2013).
38. C. Wang, F. Grillot, V. I. Kovanis, J. D. Bodyfelt, and J. Even, "Modulation properties of optically injection-locked quantum cascade lasers," Opt. Lett. **38**(11), 1975–1977 (2013).
39. B. Meng and Q. J. Wang, "Theoretical investigation of injection-locked high modulation bandwidth quantum cascade lasers," Opt. Express **20**(2), 1450–1464 (2012).

Optics EXPRESS

40. C. Harder, J. Katz, S. Margalit, J. Shacham, and A. Yariv, "Noise equivalent circuit of a semiconductor laser diode," IEEE J. Quantum Electron. **18**(3), 333–337 (1982).
41. Y. Petitjean, F. Destic, J. C. Mollier, and C. Sirtori, "Dynamic modeling of Terahertz quantum cascade lasers," IEEE J. Sel. Top. Quantum Electron. **17**(1), 22–29 (2011).
42. C. Wang, J. P. Zhuang, F. Grillot, and S. C. Chan, "Contribution of off-resonant states to the phase noise of quantum dot lasers," Opt. Express **24**(26), 29872–29881 (2016).
43. F. Capasso, R. Paiella, R. Martini, R. Colombelli, C. Gmachl, T. L. Myers, M. S. Taubman, R. M. Williams, C. G. Bethea, K. Unterrainer, H. Y. Hwang, D. L. Sivco, A. Y. Cho, A. M. Sergent, H. C. Liu, and E. A. Whittaker, "Quantum cascade lasers: Ultrahigh-speed operation, optical wireless communication, narrow linewidth, and far-infrared emission," IEEE J. Quantum Electron. **38**(6), 511–532 (2002).
44. J. Ohtsubo, *Semiconductor Lasers: Stability, Instability, and Chaos* (Springer, 2007).
45. C. Henry, "Theory of the linewidth of semiconductor lasers," IEEE J. Quantum Electron. **18**(2), 259–264 (1982).
46. J. Kim, M. Lerttamrab, S. L. Chuang, D. L. Sivco, F. Capasso, and A. Y. Cho, "Theoretical and experimental study of optical gain and linewidth enhancement factor of type-I quantum-cascade lasers," IEEE J. Quantum Electron. **40**(12), 1663–1674 (2003).
47. J. von Staden, T. Gensty, W. Elsässer, G. Giuliani, C. Mann, and C. Mann, "Measurements of the α factor of a distributed-feedback quantum cascade laser by an optical feedback self-mixing technique," Opt. Lett. **31**(17), 2574–2576 (2006).
48. T. Aellen, R. Maulini, R. Terazzi, N. Hoyler, M. Giovannini, J. Faist, S. Blaser, and L. Hvozdara, "Direct measurement of the linewidth enhancement factor by optical heterodyning of an amplitude-modulated quantum cascade laser," Appl. Phys. Lett. **89**(9), 091121 (2006).
49. L. Jumpertz, F. Michel, R. Pawlus, W. Elsäßer, K. Shires, M. Carras, and F. Grillot, "Measurements of the linewidth enhancement factor of mid-infrared quantum cascade lasers by different optical feedback techniques," AIP Adv. **6**(1), 015212 (2016).
50. T. Liu, K. E. Lee, and Q. J. Wang, "Importance of the microscopic effects on the linewidth enhancement factor of quantum cascade lasers," Opt. Express **21**(23), 27804–27815 (2013).
51. M. F. Pereira, "The linewidth enhancement factor of intersubband lasers: From a two-level limit to gain without inversion conditions," Appl. Phys. Lett. **109**(22), 222102 (2016).
52. K. Kikuchi, "Effect of 1/f-type FM noise on semiconductor-laser linewidth residual in high-power limit," IEEE J. Quantum Electron. **25**(4), 684–688 (1989).
53. A. Hangauer and G. Wysocki, "Gain compression and linewidth enhancement factor in mid-IR quantum cascade lasers," IEEE J. Sel. Top. Quantum Electron. **21**(6), 1200411 (2015).
54. L. Jumpertz, F. Michel, R. Pawlus, W. Elsäßer, M. Carras, K. Shires, and F. Grillot, "Linewidth broadening factor and gain compression in quantum cascade lasers," Proc. SPIE **9755**, 97550F (2016).

1. Introduction

Quantum cascade lasers (QCLs) are intersubband semiconductor light sources emitting in the spectral range of mid-infrared (MIR) and terahertz (THz) [1,2]. The spectrum covers the molecular "fingerprints" of many gases like nitric oxide (NO), carbon dioxide (CO_2), methane (CH_4), and hence enables various gas sensing applications [3,4]. In addition, QCLs are promising laser sources for high-resolution spectroscopy [5,6], terahertz imaging [7], and free-space optical communications as well [8,9]. However, optical noise in QCLs including the relative intensity noise and the frequency/phase noise (FN) limits the sensitivity and the resolution for the above applications [10,11]. In comparison with interband semiconductor lasers, the relative intensity noise of QCLs does not exhibit any resonance peak owing to the ultra-fast carrier lifetimes (around 1.0 ps) [12]. In addition, it decreases more slowly with increasing optical power than that in interband lasers [13–15]. In order to suppress the relative intensity noise of QCLs, researchers have resorted to the optical injection and the optical feedback techniques [16–18].

The FN in semiconductor lasers consists of the spontaneous emission noise, the carrier generation and recombination noise, as well as the low-frequency flicker noise (*1/f* noise), all of which determine the total spectral linewidth [19]. The former two noise sources are white noise and govern the lasers' intrinsic spectral linewidth, which is broadened by the linewidth broadening factor (LBF) [20]. QCLs usually exhibit near-zero LBFs, leading to narrow intrinsic linewidth in the range of 0.1–1.0 kHz [21–23]. However, the latter flicker noise arising from the current source, the thermal fluctuation, and the *internal electrical noise* considerably broadens the total spectral linewidth of QCLs to the sub-MHz or MHz range [24–26]. In order to narrow the spectral linewidth of QCLs, a large variety of frequency stabilization schemes have been proposed, including electronic feedback to the current source

[27], locking to an optical cavity [28], phase locking to a narrow-linewidth laser source [29], as well as the popular optical injection locking to an optical frequency comb [30,31]. On the other hand, there are only few theoretical studies on the FN characteristics of QCLs. M. Yamanishi *et al.* derived an analytical formula of the intrinsic linewidth of QCLs by introducing the concept of *effective coupling efficiency* of the spontaneous emission [32]. In addition, it was demonstrated that the *noisy stimulated emission* due to thermal photons considerably broadens the intrinsic linewidth of THz QCLs [33,34]. T. Liu *et al.* reported the fundamental FN caused by intrinsic temperature fluctuations in QCLs, and developed a quantum mechanical Langevin model for the calculation of the intrinsic linewidth [35,36]. In this work, we theoretically investigate the FN characteristics of QCLs through a three-level rate equation model, which includes all the Langevin noise sources for the carriers, the photon, and the phase of the electric field. It is found that the power spectral density of the FN exhibits a broad peak due to the carrier noise induced carrier variation of the upper laser level. In addition, the intrinsic linewidth of QCLs is analytically obtained through the FN analysis. It is proved that the intrinsic linewidth can be narrowed by reducing the gain coefficient or/and increasing the carrier scattering rates of the upper and the lower laser levels.

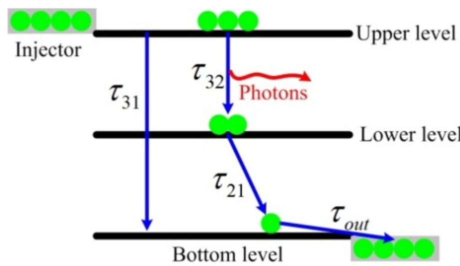

Fig. 1. Schematic of three-level electronic structure of QCLs.

2. Rate equation model with Langevin noise sources

The rate equations are developed based on the three-level electronic structure of QCLs [37–39]. As shown in Fig. 1, carriers are injected into the upper laser level of the gain region from the injector region by resonant tunneling [2]. From the upper laser level, carriers are scattered into the lower laser level with a time constant τ_{32}, and into the bottom level with a time τ_{31} through longitudinal-optical phonon emissions [2]. The stimulated emission is enabled by the population inversion between the upper and the lower laser levels. Carriers in the lower laser level scatter into the bottom level with a time τ_{21}, and finally escape the gain region with a time τ_{out} into the subsequent injector and gain stages. Accordingly, the rate equations describing the carrier numbers in the upper level (N_3), in the lower level (N_2), and in the bottom level (N_1), the photon number (S), and the phase of the electric field (ϕ) are given by

$$\frac{dN_3}{dt} = \eta\frac{I}{q} - \frac{N_3}{\tau_{32}} - \frac{N_3}{\tau_{31}} - G_0 S\Delta N + F_3(t) \tag{1}$$

$$\frac{dN_2}{dt} = \frac{N_3}{\tau_{32}} - \frac{N_2}{\tau_{21}} + G_0 S\Delta N + F_2(t) \tag{2}$$

$$\frac{dN_1}{dt} = \frac{N_3}{\tau_{31}} + \frac{N_2}{\tau_{21}} - \frac{N_1}{\tau_{out}} + F_1(t) \tag{3}$$

$$\frac{dS}{dt} = \left(mG_0\Delta N - \frac{1}{\tau_p}\right)S + m\beta\frac{N_3}{\tau_{sp}} + F_S(t) \tag{4}$$

Optics EXPRESS

$$\frac{d\phi}{dt} = \frac{\alpha_H}{2}\left(mG_0\Delta N - \frac{1}{\tau_p}\right) + F_\phi(t) \tag{5}$$

where I is the pump current, η is the current injection efficiency, G_0 is the gain coefficient, and ΔN is the population inversion given by $\Delta N = N_3$-N_2. τ_p is the photon lifetime, τ_{sp} is the spontaneous emission lifetime, β is the spontaneous emission factor, α_H is the LBF, and m is number of gain stages. The time averages of all the carrier ($F_{3,2,1}$), photon (F_S), and phase (F_ϕ) Langevin noise sources are zero due to their random nature [40]. Following the method in [20], the auto- and cross-correlations of the noise sources are derived as

$$\left\langle F_i(t)F_j(t')\right\rangle = U_{ij}\delta(t-t') \tag{6}$$

with

$$\begin{aligned}
&U_{33} = 2(G_0N_3S + N_3/\tau_{32} + N_3/\tau_{31});\ U_{22} = 2(G_0N_3S + N_3/\tau_{32})\\
&U_{SS} = 2m(G_0N_3S + \beta N_3/\tau_{sp});\ U_{\phi\phi} = 2m(G_0N_3S + \beta N_3/\tau_{sp})/(4S^2)\\
&U_{32} = -(G_0N_3S + G_0N_2S + N_3/\tau_{32});\ U_{3S} = -(G_0N_3S + G_0N_2S + \beta N_3/\tau_{sp})\\
&U_{2S} = (G_0N_3S + G_0N_2S + \beta N_3/\tau_{sp});\ U_{3\phi} = U_{2\phi} = U_{S\phi} = 0
\end{aligned} \tag{7}$$

where correlations related to F_1 are not listed, since F_1 is not involved in the FN of QCLs as expressed in Eq. (11). It is remarked that the correlations in Eq. (7) are identical to those in [13], where the phase correlations were not reported.

The small-signal Langevin noise sources perturb the laser system away from its steady-state condition, and the responses of the carriers, the photons and the phase are given by

$$\delta N_{3,2,1}(t) = n_{3,2,1}e^{j\omega t};\ \delta S(t) = se^{j\omega t};\ \delta\phi(t) = \varphi e^{j\omega t} \tag{8}$$

with ω being the angular frequency. Taking the differentials of the rate Eqs. (1)-(5) and using Eq. (8), the differential rate equations in the frequency domain are obtained as

$$\begin{bmatrix} j\omega+\gamma_{11} & -\gamma_{12} & 0 & \gamma_{14} & 0\\ -\gamma_{21} & j\omega+\gamma_{22} & 0 & -\gamma_{24} & 0\\ -\gamma_{31} & -\gamma_{32} & j\omega & 0 & 0\\ -\gamma_{41} & \gamma_{42} & 0 & j\omega+\gamma_{44} & 0\\ -\gamma_{51} & \gamma_{52} & 0 & 0 & j\omega \end{bmatrix} \begin{bmatrix} n_3(\omega)\\ n_2(\omega)\\ n_1(\omega)\\ \mathrm{s}(\omega)\\ \varphi(\omega) \end{bmatrix} = \begin{bmatrix} F_3(\omega)\\ F_2(\omega)\\ F_1(\omega)\\ F_s(\omega)\\ F_\phi(\omega) \end{bmatrix} \tag{9}$$

with

$$\begin{aligned}
&\gamma_{11} = G_0S + 1/\tau_{32} + 1/\tau_{31};\ \gamma_{12} = G_0S;\ \gamma_{14} = G_0\Delta N\\
&\gamma_{21} = G_0S + 1/\tau_{32};\ \gamma_{22} = G_0S + 1/\tau_{21};\ \gamma_{24} = G_0\Delta N\\
&\gamma_{31} = 1/\tau_{31};\ \gamma_{32} = 1/\tau_{21};\ \gamma_{41} = mG_0S + m\beta/\tau_{sp}\\
&\gamma_{42} = mG_0S;\ \gamma_{44} = 1/\tau_p - mG_0\Delta N\\
&\gamma_{51} = m\alpha_H G_0/2;\ \gamma_{52} = m\alpha_H G_0/2
\end{aligned} \tag{10}$$

Following Cramer's rule, the FN of QCLs is calculated by

$$FN(\omega) = \left|j\omega\varphi/(2\pi)\right|^2 \tag{11}$$

It is remarked that the above model is suitable for both MIR and THz QCLs to investigate the FN originating from the carrier noise and the spontaneous emission noise. However, it does

Optics EXPRESS

not include the thermal photon contribution in THz QCLs and the flicker noise in either laser, which is beyond the scope of this paper and will be studied in future work.

3. Results and discussion

The QCL parameters used for the simulations are listed in Table 1 [41], unless stated otherwise. The QCL under study exhibits a lasing threshold current of I_{th} = 222 mA. We first investigate the power spectral density of the FN, and then discuss the intrinsic spectral linewidth of the QCL.

Table 1. QCL material and optical parameters.

Symbol	Description	Value
G_0	Gain coefficient	5.3×10^4 /s
τ_p	Photon lifetime	3.7 ps
τ_{sp}	Spontaneous emission time	7.0 ns
β	Spontaneous emission factor	1.0×10^{-6}
α_H	Linewidth broadening factor	0.5
m	Gain stage number	30
τ_{32}	Scattering time upper to lower	2.0 ps
τ_{31}	Scattering time upper to bottom	2.4 ps
τ_{21}	Scattering time lower to bottom	0.5 ps
τ_{out}	Tunneling out time	0.5 ps

3.1 Power spectral density of the frequency noise

Figure 2 shows the power spectral densities of the FN (solid lines) for the QCL biased at 1.5 × I_{th}, 2.0 × I_{th}, and 5.0 × I_{th}, respectively. Like interband lasers, the FN exhibits a plateau at both low frequencies (<1.0 GHz) and high frequencies (>10 THz), and it decreases with the pump current [20]. Surprisingly, the FN exhibits a peak, which is much broader than the common resonance peak in interband lasers [42], and the peak frequency increases with the pump current. In contrast, the relative intensity noise and the intensity modulation response of QCLs do not exhibit any resonance peak [14,43]. However, QCLs subject to optical injection can show a peak in the modulation response [37,38]. On the other hand, the FN peak disappears (dashed line) once the carrier noise $F_{1,2,3}$ in Eq. (9) is removed. This phenomenon suggests that the FN peak is due to the carrier noise in the upper and the lower laser levels, since the carrier noise in the bottom level does not contribute to the FN. The significant role of the carrier noise in QCLs differs from that in interband lasers, which is usually negligible in comparison with the spontaneous emission noise [44].

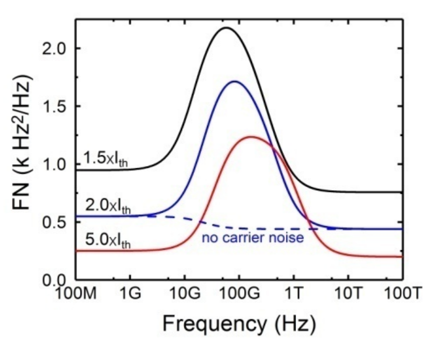

Fig. 2. FN spectra at various pump currents. The dashed line is without carrier noise at 2.0 × I_{th}.

The FN behavior can be understood through the Bode plot analysis, which describes the response of a system in the frequency domain using its zeros and poles [44]. Table 2 lists the zeros and the poles of the FN in Eq. (11) for the QCL biased at 2.0 × I_{th}. With the carrier noise, the smallest zero z_3 (non-zero absolute value) is less than the smallest pole p_3, leading to the appearance of the peak in Fig. 2. In contrast, z_3 becomes larger than p_3 without the carrier noise, resulting in the vanishing of the peak. However, there is no complex conjugate pair of poles in either case, proving that the FN exhibits no resonance.

Table 2. Zeros and poles of the FN at 2.0 × I_{th}

Carrier noise	Zeros (10^{11} Hz)				Poles (10^{11} Hz)			
	z_1, z_2	z_3	z_4	z_5	p_1, p_2	p_3	p_4	p_5
Yes	0	-0.12	-1.9	-9.5	0	-0.23	-1.7	-5.1
No	0	-0.25	-1.7	-5.1				

Because the phase of the electric field is partly determined by the population inversion as expressed in Eq. (5), the physical origin of the FN peak can be explored by examining the small-signal carrier responses, which are defined as the square of the amplitude of the carrier variations $|n_{3,2,1}(\omega)|^2$ in the frequency domain. Figure 3 presents that the carrier response of the upper laser level (n_3) exhibits a peak while that of the lower laser level (n_2) does not, which leads to the appearance of the peak in the population inversion (n_3–n_2). The peak frequency of the population inversion is the same as that of the FN in Fig. 2. An analytical analysis shows that the peak frequency is related to the stimulated emission through the rate G_0S (1.2×10^{11} Hz at $2.0 \times I_{th}$) in Eq. (1), similar to the resonance frequency of interband lasers [20]. Following the discussions in Fig. 2 and in Table 2, the FN peak can be attributed to the carrier noise induced carrier variation of the upper laser level, which is enhanced by the stimulated emission process. However, deeper physical insights of the interaction process between the carrier variation and the stimulated emission process are still required in future work.

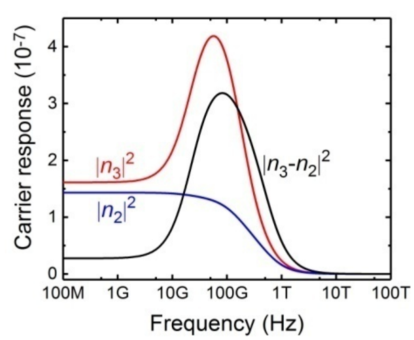

Fig. 3. Carrier responses due to the noise perturbation at 2.0 × I_{th}.

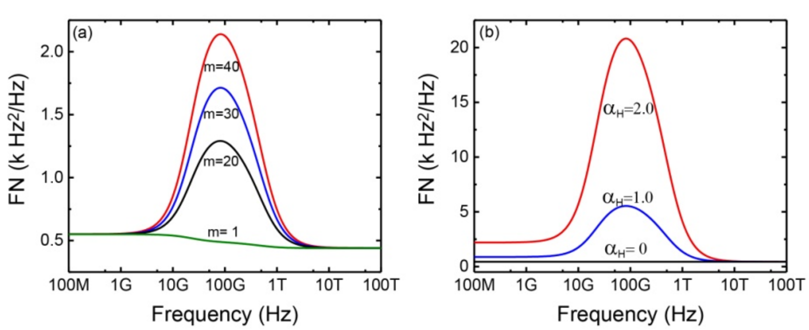

Fig. 4. (a) FN spectra with various gain stage numbers, and (b) with various LBFs at 2.0 × I_{th}.

Figure 4(a) illustrates that a QCL with fewer gain stages exhibits a lower FN peak, and the peak is almost completely suppressed for only one gain stage. However, the gain stage number does not affect the low- or high-frequency part of the FN. The LBF in semiconductor lasers describes the phase-amplitude coupling effects of the refractive index and the gain, which enhances the low-frequency FN and thereby broadens the spectral linewidth [45]. Owing to the nearly symmetric homogeneous gain broadening of the intersubband transition, QCLs operating below the lasing threshold usually show near-zero LBFs [46], while QCLs operating above threshold show higher values ranging from 0.2 to 3.0 [47–49]. The non-zero LBF in QCLs has been attributed to the non-parabolicity of the band structure, the many-body effects, the resonant tunneling transport, and the counter-rotating wave contribution [50,51]. Figure 4(b) points out that the peak of the FN is strongly dependent on the LBF value. For a LBF of zero, the FN is constant over the whole frequency range because the carrier noise and the spontaneous emission noise are white, while the flicker noise is not taken into account. On the other hand, a non-zero LBF substantially raises the peak amplitude as well as the low-frequency FN, which determines the intrinsic spectral linewidth of QCLs as discussed in the following section.

3.2 Intrinsic spectral linewidth of the quantum cascade laser

For interband lasers, the intrinsic spectral linewidth is given by the well-known formula [20]

$$\Delta v_{IL}^{D} = \left(\frac{v_g^2 \alpha_T \alpha_m}{4\pi P_0} n_{sp} h\upsilon \right) \left(1 + \alpha_H^2\right) \tag{12}$$

where P_0 is the output power, v_g is the group velocity of light, α_T is the total cavity loss, α_m is the mirror loss, n_{sp} is the population inversion factor, and $h\upsilon$ is the photon energy. The first term on the right hand of the formula gives the Schawlow-Townes linewidth limit, and the second term suggests that the LBF broadens the laser linewidth.

For QCLs, the Schawlow-Townes limit can be obtained from its high-frequency FN plateau in Fig. 2, and from Eq. (11) we derive

$$\begin{aligned} \Delta v_{ST}^{C} &\equiv 2\pi FN(\omega \to \infty) \\ &= mN_3 \frac{G_0 S + \beta / \tau_{sp}}{4\pi S^2} \approx \frac{mG_0 N_3}{4\pi S} \end{aligned} \tag{13}$$

On the other hand, the intrinsic spectral linewidth is determined by the low-frequency FN plateau as

$$\begin{aligned} \Delta v_{IL}^{C} &\equiv 2\pi FN(\omega \to 0) \\ &= \Delta v_{ST}^{C} \left(1 + \alpha_{\mathrm{H}}^2\right) \approx \frac{mG_0 N_3}{4\pi S} \left(1 + \alpha_{\mathrm{H}}^2\right) \end{aligned} \tag{14}$$

Using the steady-state solutions of the rate equations, Eq. (14) can be re-expressed as a function of the output power P_0 or the pump current I_0

$$\Delta v_{IL}^{C} = \frac{v_g \alpha_T G_0}{4\pi} \frac{\tau_{32}}{\tau_{32} - \tau_{21}} \left(\frac{h\nu v_g \alpha_m}{G_0 P_0} + \tau_{21} \right) \left(1 + \alpha_H^2\right) \tag{15a}$$

$$\Delta v_{IL}^{C} = \frac{v_g \alpha_T G_0}{4\pi} \frac{\eta_\tau^{-1}}{\tau_{32}^{-1} + \tau_{31}^{-1}} \left(\frac{1}{I_0 / I_{th} - 1} + 1 - \eta_\tau \right) \left(1 + \alpha_H^2\right) \tag{15b}$$

with

Optics EXPRESS

$$\begin{aligned}\eta_\tau &= \frac{\tau_{31}(\tau_{32}-\tau_{21})}{\tau_{32}(\tau_{31}+\tau_{21})}\\ I_{th} &= \frac{\tau_{32}+\tau_{31}}{\tau_{31}(\tau_{32}-\tau_{21})}\frac{q}{\eta}\frac{v_g\alpha_T}{mG_0}\end{aligned} \tag{16}$$

Equation (15) clearly shows that increasing the pump current or the output power reduces the laser linewidth. When the pump current is high enough, the intrinsic linewidth of QCLs eventually saturates at a minimum level

$$\Delta v^{C}_{IL\min} = \frac{v_g\alpha_T G_0}{4\pi}\frac{\tau_{32}\tau_{21}}{\tau_{32}-\tau_{21}}\left(1+\alpha_H^2\right) \tag{17}$$

In contrast, the intrinsic linewidth of interband lasers does not have this kind saturation behavior (see Eq. (12)), although external flicker noises can saturate or even rebroaden the total spectral linewidth [52]. Equation (17) is in agreement with that in [32], where the laser linewidth was derived using the Einstein relationship of the stimulated emission and the spontaneous emission. According to Eq. (15), the laser linewidth is not affected by the gain stage number as shown in Fig. 4(a), where the stage number does not modify the low-frequency FN. In contrast, a QCL with more gain stages exhibits a higher relative intensity noise [14].

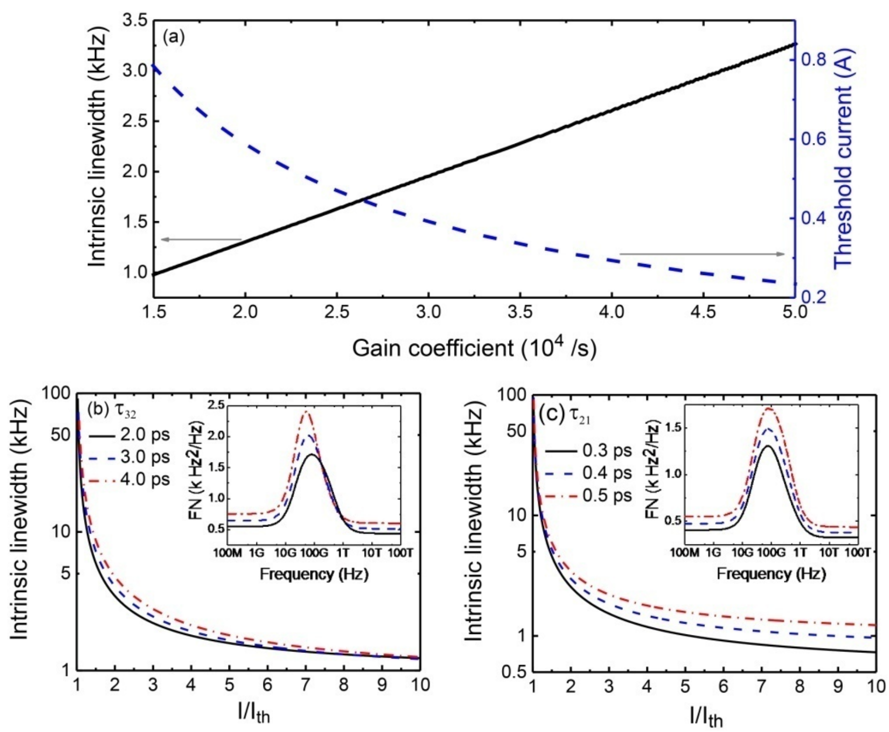

Fig. 5. Effects of (a) the gain coefficient G_0, (b) scattering time τ_{32} and (c) scattering time τ_{21} on the intrinsic linewidth. The pump current for (a) and for the insets of (b) and (c) is $2.0 \times I_{th}$.

Figure 5(a) shows that the intrinsic linewidth (solid line) of the QCL can be narrowed through reducing the gain coefficient. However, this is achieved at the cost of increasing the lasing threshold (dashed line). Equation (15) suggests that the intrinsic linewidth is dependent on the carrier scattering times. Indeed, a short time τ_{32} in Fig. 5(b) and a short time τ_{21} in Fig.

Optics EXPRESS

5(c) reduce the laser linewidth. At 5.0 × I_{th}, the linewidth slightly decreases from 1.8 kHz for τ_{32} = 4.0 ps to 1.6 kHz for τ_{32} = 2.0 ps, while it is reduced by about 40% from 1.6 kHz for τ_{21} = 0.5 ps to 1.0 kHz for τ_{21} = 0.3 ps. Therefore, the laser linewidth of QCLs can be effectively narrowed through accelerating the carrier scattering rate of the lower laser level. In addition, the FN peak amplitude is suppressed by the short scattering times as shown in the inset of Figs. 5(b) and 5(c). Finally, it is remarked that the reduction of G_0 and τ_{32} can also degrade the maximum available laser power and the dynamic performance such as the modulation bandwidth and the frequency chirp [20]. Therefore, there is a tradeoff in designing the gain coefficient and the carrier scattering times for achieving narrow-linewidth QCLs.

4. Conclusions

In conclusion, the FN characteristics and the intrinsic linewidth of QCLs have been modeled through a set of coupled rate equations including both the carrier noise and the spontaneous emission noise. It is found that the power spectral density of the FN exhibits a broad peak due to the stimulated-emission enhanced carrier variation of the upper laser level, which is driven by the carrier noise in both the upper and the lower laser levels. The peak amplitude is strongly dependent on the gain stage number and the LBF. In addition, we derive an analytical formula for the intrinsic linewidth of QCLs based on the FN analysis. It is proven that the laser linewidth can be narrowed by reducing the gain coefficient and/or accelerating the carrier scattering times of the upper and lower laser levels. In future work, we will include the thermal photon contribution to the FN of THz QCLs in the model, and design experiments to verify the theoretical predictions. In addition, recent work in [53,54] pointed out that the gain nonlinearity affected the performance of QCLs as for interband lasers. As such, the gain compression effects on the FN will be studied as well.

Funding

Shanghai Pujiang Program (17PJ1406500).

Acknowledgments

The authors would like to thank Dr. Benjamin Lingnau at Technische Universität Berlin, Germany for fruitful discussions.